

Article

An Energy-Efficient Scheme Design for NOMA-Based UAV-Assisted MEC Systems

Shanshan Wang ¹  and Zhiyong Luo ^{1,2,*} 

¹ School of Electronics and Communication Engineering, Sun Yat-sen University, Shenzhen 518107, China; wangshsh58@mail2.sysu.edu.cn

² Peng Cheng Laboratory, Shenzhen 518055, China

* Correspondence: luozhy57@mail.sysu.edu.cn

Abstract: UAV-assisted MEC networks provide extensive communication coverage and massive computation services for mobile terminals (MTs), which are considered a promising edge paradigm to support future air-ground integrated communications. In this paper, an energy-efficient scheme in NOMA-based UAV-assisted MEC systems is proposed to address the system's energy constraints and its inability to support massive MT access. Our goal is to minimize system-weighted energy consumption by jointly optimizing the allocation of transmission power, computation resources, and UAV trajectory scheduling. As the formulated problem is non-convex and difficult to solve directly, we decompose it into two manageable sub-problems and propose an iterative algorithm based on successive convex approximations (SCA) to solve each sub-problem alternatively. Simulation results show that the proposed joint optimization algorithm achieves a significant performance improvement compared to other benchmark approaches.

Keywords: MEC; UAV-assisted; NOMA; resource allocation; trajectory scheduling



Citation: Wang, S.; Luo, Z. An Energy-Efficient Scheme Design for NOMA-Based UAV-Assisted MEC Systems. *Electronics* **2024**, *13*, 4240. <https://doi.org/10.3390/electronics13214240>

Academic Editors: Yunda Yan, Dewei Yi, Hao Lu and Lan Gao

Received: 13 September 2024

Revised: 28 October 2024

Accepted: 28 October 2024

Published: 29 October 2024



Copyright: © 2024 by the authors. Licensee MDPI, Basel, Switzerland. This article is an open access article distributed under the terms and conditions of the Creative Commons Attribution (CC BY) license (<https://creativecommons.org/licenses/by/4.0/>).

1. Introduction

With the rapid development of emerging applications such as virtual/augmented reality, the Internet of Vehicles (IoV), and natural language processing, there is a growing need for wireless networks to meet stricter requirements in terms of delay and reliability [1–3]. These applications typically generate computation-intensive and delay-sensitive tasks, resulting in an explosive growth of mobile data streams [4,5]. However, the limited computing power and electrical energy of mobile terminals (MTs) are insufficient to meet the current communication and computation demands. In this context, mobile edge computing (MEC) has emerged as a promising solution that enables MTs to offload computation tasks to computing servers closer to the network edge [6]. Traditional ground network communication facilities hardly meet the communication and computation requirements in hotspots or network breakdown areas due to geographical constraints and poor flexibility. Fortunately, UAV-assisted MEC systems, as a critical component of the air-ground network, provide additional computing power for MTs due to their high mobility and flexible deployment [7]. Consequently, the development of green and energy-efficient UAV-assisted MEC systems has garnered significant attention.

Unlike ground-based MEC systems, which do not need to consider system energy consumption, UAV-assisted MEC systems face challenges such as limited onboard energy and computing power, as well as the need for additional propulsion energy to support flight [8]. Several studies have explored energy-efficient solutions for UAV-assisted MEC systems. For instance, Qi et al. [9] employed an alternating iterative optimization algorithm for joint power and trajectory scheduling in a mobile UAV network, addressing quality of service imbalances among nodes while maximizing the system's energy efficiency. Zhang et al. [10] proposed an energy-efficient resource management scheme for UAV-assisted MEC systems, designing an iterative conditional self-adaptation SCA-based algorithm to jointly optimize

offloading decisions and the allocation of communication and computation resources, ultimately achieving min–max fairness in energy consumption among UAVs. Similarly, Li et al. [11] investigated the computation offloading and trajectory planning problems from the perspectives of IoT devices and UAVs. They modeled this as a Markov decision process (MDP) and proposed a knowledge-assisted multi-agent reinforcement learning (MARL) approach to enhance system effectiveness. To address the adaptation of UAV-MEC systems to the heterogeneous needs of users, Zeng et al. [12] transformed the long-term stochastic optimization problem into two deterministic online optimization sub-problems, which were solved using the Lyapunov method. This approach effectively reduces the system's long-term energy consumption. Pan et al. [13] studied an integrated sensing and communication (ISAC) system supporting OFDMA UAVs and formulated joint trajectory planning and resource allocation problems to ensure communication service quality. UAV-assisted MEC systems hold promise for overcoming the limitations of traditional network communication, such as delay and coverage issues. However, current research still relies on traditional orthogonal multiple-access (OMA) techniques like time division multiple access (TDMA) and frequency division multiple access (FDMA). While these methods optimize resource allocation to some extent, they do not adequately address the challenges of limited spectrum resources and energy constraints related to the growing demands of large-scale MT access.

In this context, NOMA demonstrates significant advantages due to its ability to support simultaneous user access to the same time and frequency resources, making it an effective solution for UAV-assisted MEC systems [14–16]. In contrast, other spectrum efficiency enhancement techniques, such as cognitive radios, have introduced increased implementation complexity and energy overhead due to their intricate spectrum sensing and management mechanisms, which limit their applicability. Furthermore, the number of users who access ISAC technologies for practical applications is constrained by communication delays and network topology. Therefore, NOMA is more adaptable and feasible in UAV-assisted MEC systems. Diao et al. [16] proposed a joint trajectory design, task data, and computing resource allocation algorithm for NOMA-based and UAV-assisted mobile edge computing, which effectively reduced the maximum energy consumption and ensured fairness among users. Liu et al. [17] proposed a joint optimization algorithm for global computational resources and communication power to minimize system energy consumption in a UAV-assisted NOMA-MEC system, solving it using the SCA method. Liu et al. [18] proposed a joint optimization problem for UAV communication scheduling, transmit power, and motion parameters in a UAV-assisted IoT system. They solved this problem using subgradient descent and the SCA method to maximize the system's energy efficiency. Similarly, Ishan et al. [19] developed an iterative algorithm for time and computational resource allocation in a NOMA-based UAV-assisted MEC system, optimizing UAV trajectory with the SCA method. From these studies, it is evident that the SCA method effectively addresses the non-convexity and coupling inherent in optimization problems. Similarly, our proposed iterative algorithm uses the SCA method to solve each subproblem with alternating optimization to ensure optimal system performance. However, most existing literature focuses on single static UAVs and lacks in-depth studies on the effective allocation of multidimensional resources in multi-UAV cooperative systems. Additionally, many studies only consider line-of-sight (LoS) links in channel modeling, which overlooks potential link blockage in real-world applications. This can result in an inadequate assessment of communication quality and reliability between UAVs and MTs, ultimately affecting overall system performance. Furthermore, many approaches fail to address causal and temporal constraints in task offloading, limiting their ability to adapt resource allocation and scheduling strategies to dynamically changing task demands. These limitations restrict the practicality and broad applicability of current studies.

At present, research on NOMA-based UAV-assisted MEC systems is still in its early stages [20,21]. Facing the current demand for air–ground collaboration network applications, the conflict between wireless resources and computing power resources is becoming

more and more prominent, and NOMA technology can better adapt to this trend and provide efficient multi-user access solutions. Given the large-scale interconnection of MT devices generates a large amount of data, and the usual small size of MTs, limited battery life and carrying capacity challenges of UAVs, there is an urgent need to propose an energy-efficient scheme for NOMA-based UAV-assisted MEC systems in application scenarios requiring real-time responses [22,23]. While MTs use the NOMA protocol to offload computation tasks to UAVs equipped with computation servers, the introduction of NOMA introduces interference that complicates the decoding process. In addition, the limited battery capacity of the UAV limits the operating time, while the uncertain flight trajectory determines the channel gain of the link and the sequence of successive interference cancellation (SIC). This makes the proper allocation of communication and computational resources critical to the effectiveness of the system. Therefore, in order to design low-complexity and energy-efficient schemes, it is necessary to jointly optimize communication and computational resource allocation, as well as the trajectory scheduling of the UAV.

Inspired by these challenges, this paper proposes an energy-efficient scheme design for NOMA-based UAV-assisted MEC systems. Considering the limited system energy and causal and temporal constraints, we jointly optimize the allocation of transmission power and computation resources, as well as UAV trajectory scheduling, to minimize the system-weighted energy consumption. Our established system model takes into account constraints such as channel link blocking and task completion time, aiming to meet the future demands for large-scale MTs and emergency computing offloading services. The main contributions of this paper are as follows:

- The NOMA-based UAV-assisted MEC system is developed to support large-scale MT access and address urgent computational requirements. The optimization objective is to minimize the system-weighted energy consumption by jointly optimizing the allocation of transmission power, computation resources, and UAV trajectory scheduling.
- Considering that the optimization problem involves the coupling of communication resources and computing resources, it is a non-convex problem. To address this, the problem is decomposed into two sub-problems, and an efficient iterative algorithm is proposed to solve the sub-problem alternately.
- In the iterative process, the SCA method is first used to solve the optimal allocation of transmission power and computation resources by linearizing the non-convex constraints through the first-order Taylor series approximation for a given UAV trajectory. Then, the constraints on the UAV trajectory are simplified using slack variables and combined with the first-order Taylor series approximation to develop the trajectory scheduling scheme based on the allocated computation resources and transmission power. Finally, the simulation shows that the proposed optimization algorithm effectively reduces the system-weighted energy consumption compared to the benchmark scheme.

The rest of this paper is organized as follows. Section 2 describes the system model and formulates the optimization problems. In Section 3, we propose a solution to the optimization problem. The numerical results are analyzed in Section 4. Section 5 provides the conclusions and future work.

2. System Model and Problem Formulation

In this section, we present the framework for NOMA-based UAV-assisted MEC systems, which includes the system model, channel model, and energy consumption model. Additionally, we formulate the optimization problem.

2.1. System Model

As shown in Figure 1, NOMA-based UAV-assisted MEC systems consist of U UAVs and M MTs, denoted as $\mathcal{U} = \{1, 2, \dots, U\}$ and $\mathcal{M} = \{1, 2, \dots, M\}$. MTs are randomly and uniformly deployed in a defined area and all of them produce a computation-intensive task

that needs to be completed within a time interval T . For ease of analysis, the continuous computation time T can be discretized into N time slots of length $\theta = T/N$, denoted as $\mathcal{N} = \{1, 2, \dots, N\}$, where θ should be small enough to ensure that the UAV's position in each time slot is considered static [24], as illustrated in Figure 2. It is assumed that the data bits of the computation tasks are computed bit-by-bit and can be divided into different groups. Considering the limited computation capacity of MTs, we adopt a partial offloading strategy, i.e., a part of the computation tasks can be computed locally in MTs, and the other part can be simultaneously offloaded to all UAVs via the wireless link using the uplink NOMA protocol. This ensures that the amount of tasks on each UAV is relatively balanced and avoids overloading or idling certain UAVs. The computational task F_m generated by MT m is denoted as $F_m = (d_m^{mt}, f_m^{mt}, t_m^{mt})$, where d_m^{mt} is the data size of the task, f_m^{mt} is the amount of computation required by the task, and t_m^{mt} is the maximum task processing delay, respectively. UAVs equipped with MEC servers as airborne base stations are required to fly from an initial position to a final position to provide computation offloading services for MTs. Note that the NOMA protocol allows multiple MTs to share the same frequency band when offloading tasks to the same UAV node. To avoid transmission interference when MTs offload computation tasks to multiple UAVs, the FDMA protocol is used for interference management between different UAVs. Generally, MT m completes task offloading through the following processes: (1) MTs transmit their computation task to UAV through the uplink NOMA. (2) The UAV performs edge computing. (3) The UAV sends the computation results back to the MTs via downlink. Considering that the computation results are relatively small and do not consume significant system energy, the result transmission process is ignored for simplicity. UAVs do not execute edge computing in the first and last time slots, and MTs do not execute task offloading in the last time slot.

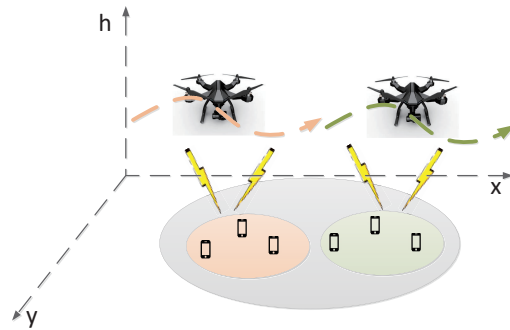


Figure 1. The NOMA-based UAV-assisted MEC systems.

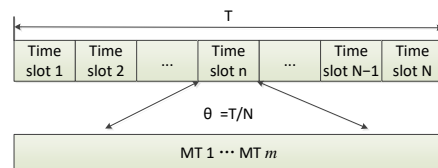


Figure 2. Time frame for task completion time T for NOMA.

A Cartesian coordinate system is established to update the position of the UAV and MT at each time slot. Setting the UAV's flight altitude as h , the location coordinates of UAV u and MT m in the n th slot are given by $\mathbf{q}_u^{\text{uav}}[n] = (x_u^{\text{uav}}[n], y_u^{\text{uav}}[n], h), u \in \mathcal{U}$ and $\mathbf{q}_m^{\text{mt}}[n] = (x_m^{\text{mt}}[n], y_m^{\text{mt}}[n], 0), m \in \mathcal{M}$, respectively. The velocity $\mathbf{v}_u[n]$ of UAV u in the n th slot can be expressed by the position $\mathbf{q}_u[n]$ in the n th slot and the position $\mathbf{q}_u[n-1]$ in the $(n-1)$ th slot. $\mathbf{v}_u[n]$ should be lower than the maximum speed v_{\max} , denoted as $\mathbf{v}_u[n] = (\mathbf{q}_u[n] - \mathbf{q}_u[n-1])/\theta \triangleq D_u[n]/\theta \leq v_{\max}, n \in \mathcal{N}, u \in \mathcal{U}$. Furthermore, a certain safety distance d_u should be maintained between any two UAVs to avoid collision, which can be obtained as $\|\mathbf{q}_u[n] - \mathbf{q}_j[n]\| \geq d_u, n \in \mathcal{N}, u \neq j$.

2.2. Channel Model

In the NOMA-based UAV-assisted MEC systems, the air-to-ground channel model between UAVs and MTs is provided by the 3GPP specification version [25]. Considering post-disaster rescue scenarios where obstacles might obstruct the UAVs-MTs links, we adopt an air-ground channel model that incorporates probabilistic averaging of the LoS and NLoS links [26,27]. Thus, the average path loss $\bar{L}_{m,u}[n]$ and the channel gain $g_{m,u}[n]$ can be expressed as follows:

$$\bar{L}_{m,u}[n] = P_{\text{LoS}}^{m,u}[n]L_{\text{LoS}}^{m,u} + P_{\text{NLoS}}^{m,u}[n]L_{\text{NLoS}}^{m,u}, \quad (1)$$

$$g_{m,u}[n] = 10^{-\bar{L}_{m,u}[n]/10}, \quad (2)$$

where $P_{\text{LoS}}^{m,u}[n]$ and $P_{\text{NLoS}}^{m,u}[n]$ represent the probabilities of LoS and NLoS conditions between MT m and UAV u in the n th time slot, respectively. $L_{\text{LoS}}^{m,u}$ and $L_{\text{NLoS}}^{m,u}$ denote the path loss for LoS and NLoS conditions.

2.3. Energy Consumption Model

In NOMA-based UAV-assisted MEC systems, a critical metric that affects the system's sustainability is energy consumption. This consumption is comprised of three main components: (1) computation energy consumption, (2) communication offloading energy consumption, and (3) UAV propulsion energy consumption.

2.3.1. Computation Energy Consumption

Since the communication and computation units of MTs are separate, MTs can perform local computing while offloading tasks to UAVs to perform edge computing [28]. In the computation model, MTs and UAVs use the dynamic frequency scaling (DFS) technique to adjust the CPU frequency at each time slot, which can be denoted as $c_m^{\text{mt}}[n] = \rho_k I_m^{\text{mt}}[n]/\theta$, $c_{m,u}^{\text{uav}}[n] = \rho_k I_{m,u}^{\text{uav}}[n]/\theta$. Here, $I_m^{\text{mt}}[n]$ and $I_{m,u}^{\text{uav}}[n]$ denote the number of computation task bits on MT m and UAV u in time slot n , respectively, and ρ_k is the task computation density. Thus, the local computing energy consumption and the edge computing energy consumption over all time slots can be expressed as follows:

$$\begin{cases} E_c^{\text{mt}} = \sum_{m=1}^M \sum_{n=1}^N \gamma_\theta (c_m^{\text{mt}}[n])^3 \theta \\ E_c^{\text{uav}} = \sum_{u=1}^U \sum_{m=1}^M \sum_{n=1}^N \gamma_\mu (c_{m,u}^{\text{uav}}[n])^3 \theta, \end{cases} \quad (3)$$

where γ_θ and γ_μ are the effective switching capacitance coefficients for the MT and UAV, respectively, which depend on the chip architecture of their processors.

2.3.2. Communication Offloading Energy Consumption

To avoid interference when computation tasks are offloaded to multiple UAVs, FDMA is used to allocate different frequency bands to each UAV. This ensures that only MTs offloaded to the same UAV will interfere with each other [29]. Without loss of generality, we rank the MTs occupying the same frequency band in each time slot based on channel gain, denoted as $g_{j_1,u}[n] \geq g_{j_2,u}[n] \geq \dots \geq g_{j_k,u}[n]$. Here, $j_k, u[n] \in U$ denotes the channel gain index value of the k th smallest MT offloaded to UAV u in the n th time slot.

In each time slot, the SIC technique based on NOMA is utilized to demodulate signals from multiple MTs in the uplink power domain. Specifically, MTs are first ranked by received signal strength. The signal with the highest strength is decoded first, while the remaining signals are treated as interfering signals. The decoded signal is then removed from the superimposed signal, and the process continues with the next strongest signal. Thus, the transmission rate of MT $j_k, u[n]$ offloaded to the UAV u in the n th slot is given by the following:

$$R_{j_k,u}[n] = B \log_2 \left(1 + \frac{p_{j_k,u}[n] g_{j_k,u}[n]}{\sum_{l=1}^{k-1} p_{j_l,u}[n] g_{j_l,u}[n] + \sigma^2} \right) \theta, \quad (4)$$

where B represents the channel bandwidth allocated to each UAV, $p_{j_k,u}[n]$ represents the transmission power of MT j_k for offloading tasks to UAV u , and σ^2 represents the white Gaussian noise power.

To ensure the successful offloading of the computation task, the condition $R_{j_k,u}[n] \geq d_m^{\text{mt}} / t_m^{\text{mt}}$ must be satisfied. Therefore, the communication offloading energy consumption in all time slots is expressed as follows:

$$E_{\text{off}}^{\text{mt}} = \sum_{m=1}^M \sum_{n=1}^N \sum_{u=1}^U p_{m,u}[n] \theta, \quad (5)$$

2.3.3. UAV Propulsion Energy Consumption

The propulsion energy consumption of UAV u in all time slots is given by [30] and can be expressed as follows:

$$E_u^{\text{uav}} = P_1 \sum_{u=1}^U \sum_{n=1}^N \left(\sqrt{\theta^4 + \frac{D_u[n]^4}{4v_0^4}} - \frac{D_u[n]^2}{2v_0^2} \right)^{\frac{1}{2}} + \sum_{u=1}^U \sum_{n=1}^N \frac{1}{2} d_0 \rho s A \frac{D_u[n]^3}{\theta^2} + P_0 \sum_{u=1}^U \sum_{n=1}^N \left(\theta + \frac{3D_u[n]^2}{\theta U_{\text{tip}}^2} \right), \quad (6)$$

where P_0 and P_1 are the rotor profile power and induced power of UAV in hovering state, U_{tip}^2 is the tip speed of the rotor, v_0 is the average induced speed of the rotor, and d_0 and s are the fuselage drag ratio and the rotor stability. ρ and A denote the air density and rotor disc area, respectively.

In summary, the system-weighted energy consumption over time T can be defined as the weighted sum of the computation energy consumption, communication offloading energy consumption, and UAV propulsion energy consumption. This is expressed as follows:

$$\begin{aligned} E_{\text{sum}} &= \omega_{\text{mt}} (E_c^{\text{mt}} + E_{\text{off}}^{\text{mt}}) + \omega_{\text{uav}} (E_c^{\text{uav}} + \eta E_u^{\text{uav}}) \\ &= \omega_{\text{uav}} \left(\sum_{m=1}^M \sum_{u=1}^U \sum_{n=1}^N \gamma_m^{\text{uav}} (c_{m,u}^{\text{uav}}[n])^3 \theta + \eta E_u^{\text{uav}}[n] \right) \\ &\quad + \omega_{\text{mt}} \left(\sum_{u=1}^U \sum_{n=1}^N \gamma_u^{\text{mt}} (c_m^{\text{mt}}[n])^3 \theta + \sum_{m=1}^M \sum_{u=1}^U \sum_{n=1}^N p_{m,u}[n] \theta \right), \end{aligned} \quad (7)$$

where ω_{uav} and ω_{mt} are the weight factors for the energy consumption of MTs and UAVs, respectively, and satisfy $\omega_{\text{uav}} + \omega_{\text{mt}} = 1$. We can adjust the energy consumption weight factors according to the preference of the actual system for trade-off between the energy consumption of UAVs and MTs. η is the flight energy consumption coefficient used to reduce the difference in energy consumption magnitude between UAVs and MTs.

2.4. Problem Formulation

Based on the above analysis, we formulate the optimization problem P1. The goal is to minimize the system-weighted energy consumption over a time period T by jointly optimizing the allocation of transmission power \mathbf{p} and computation resources \mathbf{c}_m and \mathbf{c}_u , as well as UAV trajectory scheduling \mathbf{q}_u . The mathematical formulation is described as follows:

$$\begin{aligned}
 & \text{P1: } \min_{\mathbf{p}, \mathbf{c}_m, \mathbf{c}_u, \mathbf{q}_u} E_{\text{sum}} \\
 \text{s.t. C1: } & 0 \leq \sum_{u=1}^U p_{m,u}[n] \leq p_{\text{max}}^{\text{mt}}, \forall n, \forall m \\
 \text{C2: } & \sum_{m=1}^M c_{m,u}^{\text{uav}}[n] \leq c_{m,\text{max}}^{\text{uav}}, \forall n, \forall u \\
 \text{C3: } & 0 \leq c_m^{\text{mt}}[n] \leq c_{m,\text{max}}^{\text{mt}}, \forall m, \forall n \\
 \text{C4: } & \sum_{t=1}^{n-1} R_{m,u}[t] \geq \sum_{t=1}^n I_{m,u}^{\text{uav}}[t], \forall m \\
 \text{C5: } & \sum_{n=1}^N \sum_{u=1}^U (I_m^{\text{mt}}[n] + I_{m,u}^{\text{uav}}[n]) \geq d_m^{\text{mt}}, \forall m \\
 \text{C6: } & \sum_{t=1}^{n-1} R_{m,u}[t] \geq \sum_{t=1}^n I_{m,u}^c[t], \forall m, \forall n, \forall u \\
 \text{C7: } & (\|\mathbf{q}_u[n] - \mathbf{q}_u[n-1]\|) / \theta \leq v_{\text{max}}, \forall n, \forall u \\
 \text{C8: } & \|\mathbf{q}_u[n] - \mathbf{q}_j[n]\| \geq d_u, \forall n, u \neq j \\
 \text{C9: } & \mathbf{q}_u[0] = \mathbf{q}_{I,u}, \mathbf{q}_u[N] = \mathbf{q}_{F,u}, \forall u \\
 \text{C10: } & E_c^{\text{uav}} + \eta E_u^{\text{uav}} \leq E_{\text{uav_all}}
 \end{aligned} \tag{8}$$

In problem P1, C1 represents the limit of the uplink transmission power. C2 and C3 are the CPU cycle limits for UAVs and MTs. C4 ~ C6 describes the causal relationship between task communication transmission and offloading computation. C7 ~ C10 denotes the flight speed, location coordinates, and battery capacity limits of the UAVs. Since UAV trajectory scheduling \mathbf{q}_u is coupled with other variables, P1 is a non-convex optimization problem and is difficult to solve directly. Therefore, we propose an alternating iterative optimization algorithm to solve P1.

3. Proposed Solution

To solve the optimization problem P1, we first decouple it into two manageable sub-problems. The first sub-problem is to optimize the allocation of transmission power and computation resources, given a fixed UAV trajectory. The second sub-problem is to optimize the UAV trajectory scheduling, given a fixed allocation of transmission power and computation resources. Then, an efficient optimization algorithm is proposed to solve each sub-problem alternately using the SCA method. This involves introducing slack variables and employing Taylor series approximation techniques until the algorithm converges.

3.1. Optimize the Allocation of Transmission Power and Computation Resources

When UAV trajectory scheduling \mathbf{q}_u is fixed, P1 can be reformulated as follows:

$$\begin{aligned}
 & \text{P1.1: } \min_{\mathbf{p}, \mathbf{c}_m, \mathbf{c}_u} \omega_{\text{mt}} (E_c^{\text{mt}} + E_{\text{off}}^{\text{mt}}) + \omega_{\text{uav}} (E_c^{\text{uav}} + \eta E_u^{\text{uav}}) \\
 \text{s.t. } & \text{C1} \sim \text{C6}
 \end{aligned} \tag{9}$$

With the UAV trajectories predetermined, the UAV's propulsive energy consumption remains constant. Furthermore, We can directly observe that E_{sum} is convex with respect to \mathbf{c}_m and \mathbf{c}_u , as shown in Equation (7). However, the concavity of E_{sum} concerning the variable \mathbf{p} needs to be justified according to the equation transformation. To address this, Equation (4) is reformulated in exponential terms as follows:

$$e^{\frac{\ln 2 R_{j,k,u}[n]}{B\theta}} = 1 + \frac{p_{j,k,u}[n] g_{j,k,u}[n]}{\sum_{l=1}^{k-1} p_{j,l,u}[n] g_{j,l,u}[n] + \sigma^2} \tag{10}$$

Given that the cumulative transmitted power sum of MTs is recursive, P1.1 can be transformed into an equivalent convex function. For ease of calculation, the constant term and the denominator in Equation (10) can be defined as $N = \ln 2/B\theta$, $T_{j_k,u}[n] = \sum_{l=1}^k p_{j_l,m}[n]g_{j_l,m}[n] + \sigma^2$. Using the recursive properties of $T_{j_k,u}[n]$, we can obtain $T_{j_k,u}[n] = e^{NR_{j_k,u}[n]}T_{j_{k-1},u}[n]$. By Defining $x_{k,u}[n] = \sum_{l=1}^k R_{j_l,u}[n]$, $T_{j_k,u}[n]$ and $p_{j_k,u}[n]$ can be expressed as follows:

$$\begin{cases} T_{j_k,u}[n] = \sigma^2 e^{Nx_{k,u}[n]}, \forall u \\ p_{j_k,u}[n] = \frac{T_{j_k,u}[n] - T_{j_{k-1},u}[n]}{g_{j_k,u}[n]}, \forall u \end{cases} \quad (11)$$

The cumulative transmission power sum of all MTs is expressed as follows:

$$\begin{aligned} \sum_{k=1}^U p_{j_k,u}[n] &= \sum_{k=1}^U \frac{\sigma^2}{g_{j_k,u}[n]} \left(e^{Nx_{k,u}[n]} - e^{Nx_{k-1,u}[n]} \right) \\ &= \sigma^2 \sum_{k=0}^U \left(\frac{1}{g_{j_k,u}[n]} - \frac{1}{g_{j_{k+1},u}[n]} \right) e^{Nx_{k,u}[n]}. \end{aligned} \quad (12)$$

Considering that $g_{j_{k+1},u}[n] \geq g_{j_k,u}[n]$, the coefficients of each exponential function in Equation (12) are non-negative. Defining $\varepsilon_{k,u} = 1/g_{j_k,u}[n]$, Equation (12) can be redefined as follows:

$$\sum_{k=1}^U p_{j_k,u}[n] = \sigma^2 \sum_{k=0}^U \left[(\varepsilon_{k,u}[n] - \varepsilon_{k+1,u}[n]) e^{Nx_{k,u}[n]} \right]. \quad (13)$$

At this point, the verification of P1.1 regarding the convexity of the variable \mathbf{p} is complete. In addition, let $w_{(m,u,n)}$ denote the order in which MT m is offloaded to UAV u in the n th time slot. The amount of data transfer in the n th time slot is $R_{m,u}[n] = x_{w_{(m,u,n)},u}[n] - x_{w_{(m,u,n)}-1,u}[n]$. P1.1 is reformulated as follows:

$$\begin{aligned} \text{P1.2: } & \min_{x, \mathbf{c}_m, \mathbf{c}_u} \sigma \\ \text{s.t. } & \text{C2} \sim \text{C5} \\ \text{C1}' : & 0 \leq \sum_{u=1}^U \frac{e^{Nx_{w_{(u,m,n)},u}[n]} - e^{Nx_{w_{(u,m,n)}-1,u}[n]}}{g_{w_{(u,m,n)},u}[n]} \leq \frac{p_{\max}^m}{\sigma^2}. \\ \text{C6}' : & \sum_{t=1}^{n-1} \left(x_{w_{(m,u,t)},u}[n] - x_{w_{(m,u,t)}-1,u}[n] \right) \geq \sum_{t=1}^n I_{m,u}^c[t] \end{aligned} \quad (14)$$

In problem P1.2, C2 ~ C5, C6' are all affine transformations on variables, which are still convex constraints. However, the constraint C1' is not guaranteed to be convex; therefore, we propose to use the SCA method to transform C1' into a convex constraint through first-order Taylor series approximation, thereby converting the optimization problem P1.2 into a standard convex problem. In this process, SCA generates a solvable convex problem by performing a linear approximation of the non-convex function around the current solution, ensuring the feasibility of the constraints and the optimization of the objective function at each iteration.

If $f(x) = e^{Nx}$, it can be observed that $f(x)$ is a convex function of x . The global lower bound of a convex function is its first-order Taylor expansion, which can be obtained as $e^{Nx} \geq e^{Nx_0} + Ne^{Nx_0}(x - x_0)$. Take the above equation into C1' and reformulate P1.2 as follows:

$$\begin{aligned}
 & \text{P1.3: } \min_{x, \mathbf{c}_m, \mathbf{c}_u} \sigma \\
 & \text{s.t. } \text{C2} \sim \text{C5}, \text{C6}' \\
 & \text{C1}'' : 0 \leq \sum_{u=1}^U \frac{1}{g^{w_{(m,u,n),u}}[n]} \times \left[f\left(x_{w_{(m,u,n),u}}[n]\right) \right. \\
 & \quad \left. - \tilde{f}\left(x_{w_{(m,u,n)-1,u}}[n] \mid \hat{x}_{w_{(m,u,n)-1,u}}^{\zeta-1}[n]\right) \right] \leq \frac{p_{\max}^m}{\sigma^2}
 \end{aligned} \tag{15}$$

where $\hat{x}_{k,u}^{\zeta-1}[n]$ is the result of the $(\zeta - 1)$ th iteration for $x_{k,u}[n]$. The constraint C1'' is expressed as the difference between exponential and affine functions, so it is guaranteed to be convex, thus ensuring the convexity of P1.3. We find the solution using classical convex optimization tools like the CVX toolbox [31].

3.2. Optimize UAV Trajectory Scheduling

Given the allocation of transmission power \mathbf{p} and computation resources on the MTs and UAVs \mathbf{c}_m and \mathbf{c}_u , we aim to optimize \mathbf{q}_u , where P1 can be formulated as follows:

$$\begin{aligned}
 & \text{P2.1: } \min_{\mathbf{q}_u} E_{\text{all}} \\
 & \text{s.t. } \text{C7} \sim \text{C10}
 \end{aligned} \tag{16}$$

Considering that the allocation of transmission power \mathbf{p} and computation resources \mathbf{c}_m and \mathbf{c}_u are fixed, we only need to focus on the UAV propulsion energy consumption E_u^{uav} . The first term $P_1 \sum_{u=1}^U \sum_{n=1}^N \left(\sqrt{\theta^4 + \frac{D_u[n]^4}{4v_0^4}} - \frac{D_u[n]^2}{2v_0^2} \right)^{\frac{1}{2}}$ in E_u^{uav} is non-convex, leading to the fact that P2.1 is non-convex as well. To address this, we introduce the slack variables $f[n] = \left(\sqrt{\theta^4 + \frac{D_u[n]^4}{4v_0^4}} - \frac{D_u[n]^2}{2v_0^2} \right)^{\frac{1}{2}}$ to solve P2.1. Thus, P2.1 can be reformulated as follows:

$$\begin{aligned}
 & \text{P2.2: } \min_{\mathbf{q}_u} \omega_{\text{uav}} \eta E_u^{\text{uav}}[n] \\
 & \text{s.t. } \text{C7} \sim \text{C10} \\
 & \text{C11: } \frac{\theta^4}{f[n]^2} \leq f[n]^2 + \frac{D_u[n]^2}{v_0^2} \\
 & \text{C12: } f[n] \geq 0, n \in \mathcal{N}
 \end{aligned} \tag{17}$$

Since the right-hand side of C11 is a concave function with respect to $\mathbf{q}_u[n]$, we use the SCA method to solve it [32]. See the Appendix A for the first-order Taylor expansion of the right-hand side term of the C11 inequality, who is an affine function on $f[n]$ and $\mathbf{q}_u[n]$. $f[n]^{(l)}$ and $\mathbf{q}_u[n]^{(l)}$ are the l th iteration values of $f[n]$ and $\mathbf{q}_u[n]$, respectively. P2.2 can be reformulated as follows:

$$\begin{aligned}
 & \text{P2.3: } \min_{f[n], \mathbf{q}_u[n]} \varphi \\
 & \text{s.t. } \text{C7} \sim \text{C9}, \text{C11}, \text{C12} \\
 & \text{C10}' : \frac{\theta^4}{f[n]^2} \leq F_n^{(l)}(\mathbf{q}_u[n])
 \end{aligned} \tag{18}$$

Thus, P2.3 is transformed into a convex optimization problem, which can be solved using CVX.

3.3. Overall Algorithm Design and Analysis

By solving the two sub-problems alternately, we obtain the complete procedure of the P1, as described in Algorithm 1. In each iteration, σ_t and φ_c are monotonically non-increasing sequences of t and c , respectively, and are lower bounds of the respective sequences. Thus, the Algorithm 1 is convergent.

Algorithm 1 Iterative optimization algorithm for P1.

Input: $m, u, B, \sigma^2, U_{\text{tip}}, v_0, d_0, \sigma, s, V_{\text{max}}, \vartheta, v$
Output: $\mathbf{p}, \mathbf{c}_m, \mathbf{c}_u, \mathbf{q}_u$

- 1: Initialize $\mathbf{p}^t, \mathbf{c}_m^t, \mathbf{c}_u^t$; set iteration index $t = 1$
- 2: **repeat**
- 3: Set $\mathbf{q}_u = \mathbf{q}_u^t$ and solve P1.3 to obtain $\mathbf{p}^{t+1}, \mathbf{c}_m^{t+1}, \mathbf{c}_u^{t+1}$
- 4: Update iteration index: $t = t + 1$
- 5: Compute initial system weight energy consumption σ_0
- 6: **repeat**
- 7: Initialize $\mathbf{q}_u^c, \mathbf{c}^c$; set iteration index $c = 1$
- 8: Set $\mathbf{p} = \mathbf{p}^c, \mathbf{c}_m = \mathbf{c}_m^c$, and $\mathbf{c}_u = \mathbf{c}_u^c$, solving P2.2 to obtain \mathbf{q}_u^{c+1}
- 9: Update iteration index: $c = c + 1$
- 10: Compute system weight energy consumption φ_c
- 11: **until** $|\varphi_c - \varphi_{c-1}| \leq \nu$
- 12: **until** $|\sigma_t - \sigma_{t-1}| \leq \vartheta$

The computational complexity of Algorithm 1 depends on both the decision variables and the number of constraints in each sub-problem. According to reference [33], the computational complexity for achieving optimal accuracy μ in a convex optimization problem is $O(\log(1/\mu)n^{3.5})$, where n is the number of decision variables. The number of decision variables in two sub-problems are denoted as $n_1 = 2MUN + MN$ and $n_2 = 2U(N - 1)$, respectively. Therefore, when the number of iterations of the two sub-problems are K_1 and K_2 , respectively, the overall complexity of Algorithm 1 is denoted as $K_2(K_1O(\log(1/\mu)n_1^{3.5}) + O(\log(1/\mu)n_2^{3.5}))$.

4. Simulation Results

In this section, we will evaluate the performance of the proposed algorithm through simulation analysis. The simulation results are divided into three parts: (1) validating the convergence of the proposed algorithm; (2) comparing the differences in UAV flight trajectories and system-weighted energy consumption between the proposed algorithm in NOMA systems and the widely used OMA systems; (3) comparing the proposed algorithm to other NOMA-based resource allocation and trajectory schedule algorithms to verify its performance under various parameter configurations.

In the simulation, we consider a scenario with $m = 10$ MTs randomly distributed within a square area of $1 \times 1 \text{ km}^2$. Each MT is assigned a computation-intensive task of 150 Mb that needs to be completed within a given time period. Smaller time slot lengths can improve the smoothness, flexibility, and task efficiency of trajectory planning but also increase the computational burden. On the contrary, larger time slot lengths can simplify the computation but may lead to unsmooth trajectories and reduce the system's responsiveness to the dynamic environment. Therefore, we use a widely representative value of $T = 100 \text{ s}$ and $N = 40$ for simulation [34]. The UAV's flight altitude and maximum speed are $h = 20 \text{ m}$ and $v_{\text{max}} = 15 \text{ m/s}$, respectively. The initial and final locations of the UAV are $\mathbf{q}_{I,\mu} = [0, 0, h]$ and $\mathbf{q}_{F,\mu} = [1000, 0, h], [0, 1000, h]$. The system bandwidth is $B = 20 \text{ MHz}$. According to the principle that closer energy consumption weight factors result in lower system energy consumption [20], we set $\omega_{\text{mt}} = 0.6$ and $\omega_{\text{uav}} = 0.4$. The remaining system parameters are summarized in Table 1.

In Figure 3, the system-weighted energy consumption is depicted for different numbers of MTs to verify the algorithm's convergence, with the parameter $u = 2$. As the number of MTs increases, the complexity of NOMA decoding rises significantly, potentially impacting the algorithm's applicability in real-world scenarios. Consequently, in our initial experiments, we prioritized verifying the algorithm's convergence within a narrower interval, specifically with the number of MTs ranging from 8 to 16. This approach helps ensure the algorithm's effectiveness and practicality. It is evident from Figure 3 that the system-weighted energy consumption rises as the number of MTs increases. Initially,

the system-weighted energy consumption decreases rapidly with different numbers of MTs, eventually stabilizing at a specific value after approximately seven iterations. This observation confirms the convergence of the proposed algorithm.

Table 1. Parameter settings.

Parameters	Value
$\gamma_\mu, \gamma_\theta$	10^{-28}
θ, ν	10^{-3}
σ^2	10^{-9} W
ρ_k	10^3 cycle/bit
$c_{\max}^{\text{mt}}, c_{\max}^{\text{uav}}$	1 GHz, 10 GHz
η	10^{-4}
e	10^5 J
$a, b, \eta_{\text{LOS}}, \eta_{\text{NLOS}}$	9.16, 1.16, 1 dB, 20 dB
UAV: $P_0, P_1, U_{\text{tip}}, d_0, \rho, s$	79.9 W, 88.63 W, 120 m/s 0.6, 1.225 km ³ , 0.05 m ³

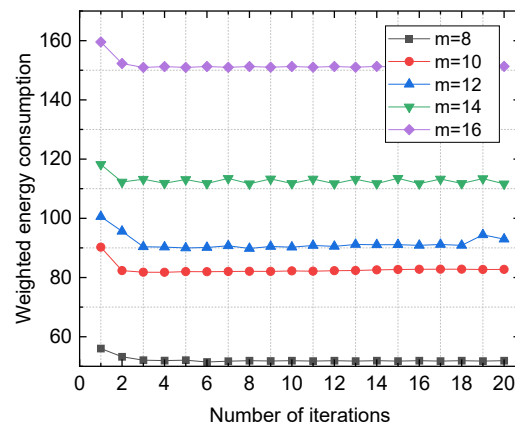


Figure 3. Convergence of the proposed algorithm under different numbers of MTs.

To validate the advantages of our proposed algorithm in NOMA systems, we selected a reference scheme, namely, OMA-RM, which adopts the classical OMA model during the offloading process and maintains the same system configuration as our proposed system [10]. In this reference scheme, joint optimization of offloading decisions, communication, and computational resource allocation is performed to minimize system energy consumption, utilizing an efficient iterative algorithm based on SCA for solution finding. This scheme is widely used in UAV communication, providing a solid basis for comparison with our proposed algorithm. Without considering the interference, the bandwidth of each MT in OMA mode is reduced to $1/m$ in NOMA mode. Therefore, the relationship between transmission rate and transmit power is as follows:

$$\begin{cases} R_{m,u}^{\text{OMA}} = \frac{B \cdot \theta}{m} \log_2 \left(1 + \frac{p_{m,u}[n] g_{m,u}[n]}{\sigma^2 / m} \right) \\ p_{m,u}^{\text{OMA}} = \frac{\sigma^2}{m g_{m,u}[n]} \left[\exp \left(\frac{m \ln 2}{B \theta} R_{m,u}[n] \right) - 1 \right] \end{cases} \quad (19)$$

We analyzed the UAV trajectories under different numbers of UAVs in both NOMA and OMA modes when $m = 10$ and $N = 40$, as shown in Figure 4. The results indicate that the UAV trajectories in both access modes are generally similar. When deploying multiple UAVs compared to a single UAV, each UAV is responsible for offloading tasks within a smaller communication range and collaborates with others to complete the offloading tasks. In contrast to the OMA mode, UAVs operating in the NOMA mode can dynamically adjust their flight paths in real-time based on user demands and the changing network topology. This allows them to approach MTs more effectively, thereby improving channel conditions

between the MTs and UAVs and significantly reducing energy consumption for uplink communication offloading. These advantages demonstrate that trajectory optimization for UAVs in the NOMA mode not only enhances system performance but also strengthens their applicability in complex environments.

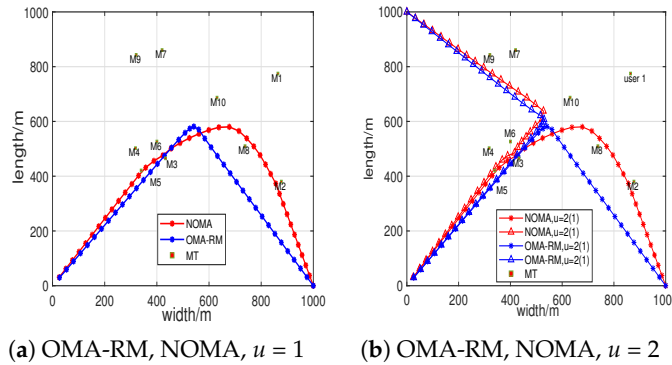


Figure 4. Flight trajectories for different numbers of UAVs.

Figure 5 further analyzes the proportion of system-weighted energy composition in both NOMA and OMA modes when $u = 2$ and $m = 10$. Specifically, there is a reduction of 18.91% in system-weighted energy consumption, 40.54% in communication offloading energy consumption, and not much difference in flight propulsion energy consumption due to the similarity of trajectories in the two modes. This is due to the fact that computation tasks prefer to perform task offloading at MEC servers with more computing power compared to local computing. In addition, more MTs in the NOMA mode will reuse the same spectrum, which makes MTs use larger bandwidth and less transmission power to accomplish task offloading, thus reducing communication offloading energy consumption.

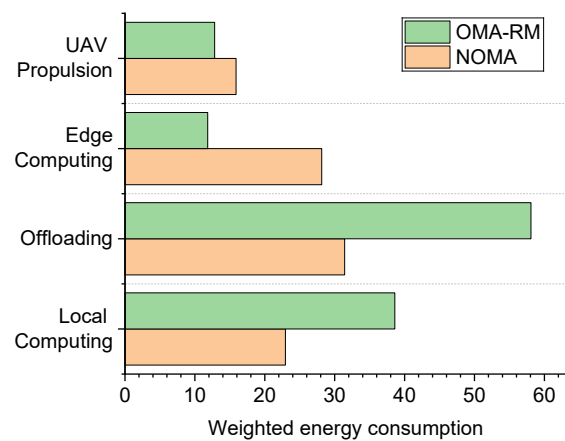


Figure 5. Weighted energy consumption composition for NOMA and OMA.

In addition, we evaluate the performance of the proposed resource allocation and trajectory optimization scheme within NOMA-based and UAV-assisted MEC systems, comparing it to two other NOMA-based benchmark schemes: a UAV fixed trajectory scheme (Fixed trajectory) [35], in which the UAV flies directly from the initial position to the endpoint, and a computational resource equivalent allocation scheme (Equal resource) [19]. Figure 6 illustrates the system-weighted energy consumption for varying numbers of MTs with $u = 2$. It is evident that the system-weighted energy consumption increases progressively with the number of MTs. Specifically, when the number of MTs reaches 14, the energy consumption of the proposed scheme is reduced by 61.9% and 43.3% compared to the fixed trajectory and equal resource schemes, respectively. In the fixed trajectory scheme, the UAV can only follow a predetermined linear path, resulting in poorer channel

conditions for MTs located off that path. This limitation causes the computation tasks to rely more heavily on local computing, ultimately leading to an increase in system-weighted energy consumption. These findings further validate that the proposed scheme effectively supports a greater number of user accesses while minimizing the system-weighted energy consumption by jointly optimizing transmission power, computational resource allocation, and UAV flight trajectory scheduling in the NOMA mode.

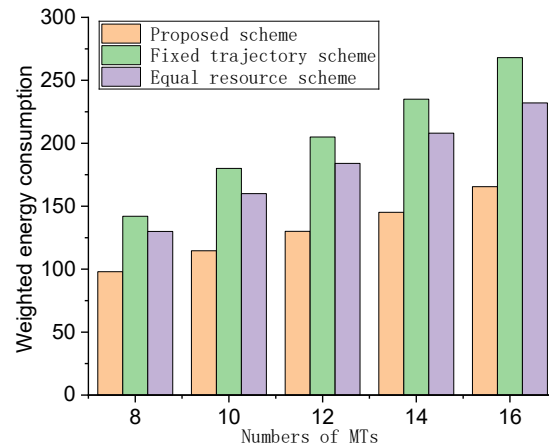


Figure 6. Weighted energy consumption versus number of MTs.

Figure 7 shows the system-weighted energy consumption of different algorithms under task completion times T when the number of UAVs is 2. We can see that the system-weighted energy consumption of each scheme shows a decreasing trend with the increase of the task completion time T . At $T = 100$ s, the system-weighted energy consumption of the proposed algorithm is reduced by 27.2% and 63.5% compared to the equal resource and fixed trajectory schemes, respectively. This is because as T increases, the proposed scheme can be more flexible in allocating the transmission power and computation resources as well as optimizing the flight trajectory scheduling, which reduces the overall energy consumption of the system. Specifically, in the case of longer task completion time T , the data transmission power can be carried out at a lower power, which reduces the transmission energy consumption. Additionally, the UAV's flight trajectory is optimized for energy savings, further decreasing flight energy consumption. These facts further confirm that our proposed joint optimization algorithm can effectively manage the balance between delay and energy consumption as task completion time increases, thus achieving a gradual reduction in system-weighted energy consumption.

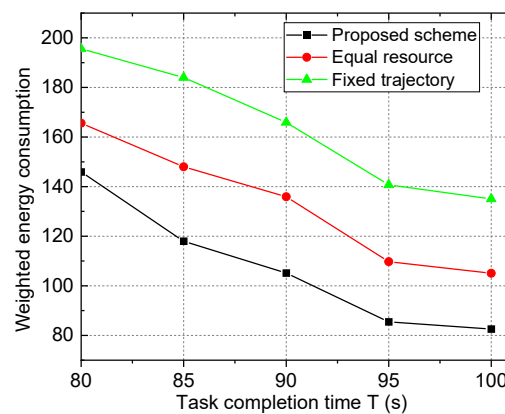


Figure 7. Weighted energy consumption versus task completion time T .

5. Conclusions

In this paper, we carry out an energy-efficient scheme design for NOMA-based UAV-assisted MEC systems, which are used to solve system energy constraints and massive MT access challenges. Our goal is to minimize the system-weighted energy consumption by jointly optimizing the allocation of transmission power and computation resources as well as UAV trajectory scheduling. Since the formulated problem is non-convex and difficult to solve directly, we design an efficient iterative algorithm using SCA. We evaluated the effectiveness of the proposed algorithm in terms of multiple dimensions such as convergence, UAV trajectory, weighted energy consumption composition, and task completion time. Simulations showed that the proposed algorithm achieved lower system-weighted energy consumption and revealed the system's trade-off between delay and energy consumption. In future work, considering the challenges of strong interference in the NOMA system and the high complexity of SIC decoding when a large number of MTs share the same channel, we will consider the study of user grouping and user group scheduling order in a hybrid multiple-access system.

Author Contributions: Conceptualization, S.W. and Z.L.; writing—original draft preparation, S.W.; writing—review and editing, Z.L. All authors have read and agreed to the published version of the manuscript.

Funding: This work was supported in part by the National Key R&D Program of China under Grant 2021YFB2900200, the Ministry of Education of China University Innovation Funds under Grant 2021ZYA05003, and the Key Natural Science Foundation of Shenzhen under Grant JCYJ20220818102209020.

Data Availability Statement: Data is contained within the article.

Conflicts of Interest: The authors declare no conflicts of interest.

Appendix A

The first-order Taylor expansion of the right-hand term of the C11 inequality can be expressed as Equation (A1). The specific derivation to the process is as follows:

$$f[n]^2 + \frac{D_u[n]^2}{v_0^2} \geq f[n]^{(l)} + 2f[n]^{(l)}(f[n] - f[n]^{(l)}) + \frac{\|\mathbf{q}_u[n+1]^{(l)} - \mathbf{q}_u[n]^{(l)}\|^2}{v_0^2} + \frac{2}{v_0^2} \left(\|\mathbf{q}_u[n+1]^{(l)} - \mathbf{q}_u[n]^{(l)}\| \right) \left(\|\mathbf{q}_u[n+1] - \mathbf{q}_u[n]\| - \|\mathbf{q}_u[n+1]^{(l)} - \mathbf{q}_u[n]^{(l)}\| \right) \triangleq F_n^{(l)}(\mathbf{q}_u[n]). \quad (\text{A1})$$

References

1. Mao, Y.; You, C.; Zhang, J.; Huang, K.; Letaief, K.B. A survey on mobile edge computing: The communication perspective. *IEEE Commun. Surv. Tutorials* **2017**, *19*, 2322–2358. [\[CrossRef\]](#)
2. Zhou, F.; Hu, R. Q.; Li, Z.; Wang, Y. Mobile Edge Computing in Unmanned Aerial Vehicle Networks. *IEEE Wirel. Commun.* **2020**, *27*, 140–146. [\[CrossRef\]](#)
3. Jiang, F.; Wang, K.; Dong, L.; Pan, C.; Xu, W.; Yang, K. AI driven heterogeneous MEC system with UAV assistance for dynamic environment: Challenges and solutions. *IEEE Netw.* **2020**, *35*, 400–408. [\[CrossRef\]](#)
4. Cruz, P.; Achir, N.; Viana, A.C. On the edge of the deployment: A survey on multi-access edge computing. *ACM Comput. Surv.* **2022**, *55*, 1–34. [\[CrossRef\]](#)
5. Zhou, E.; Liu, Z.; Lan, P.; Xiao, W.; Yang, W.; Niu, X. Interference Avoidance through Periodic UAV Scheduling in RIS-Aided UAV Cluster Communications. *Electronics* **2023**, *12*, 4539. [\[CrossRef\]](#)
6. Wang, S.; Xin, N.; Luo, Z.; Lin, T. An Efficient Computation Offloading Strategy Based on Cloud-Edge Collaboration in Vehicular Edge Computing. In Proceedings of the 2022 International Conference on Computing, Communication, Perception and Quantum Technology (CCPQT), Xiamen, China, 5–7 August 2022; IEEE: Toulouse, France, 2022; pp. 193–197.
7. Wang, L.; Zhang, H.; Guo, S.; Yuan, D. Communication-, Computation-, and Control-Enabled UAV Mobile Communication Networks. *IEEE Internet Things J.* **2022**, *9*, 20393–20407. [\[CrossRef\]](#)
8. Li, X.; Fan, R.; Hu, H.; Zhang, N. Joint Task Offloading and Resource Allocation for Cooperative Mobile-Edge Computing Under Sequential Task Dependency. *IEEE Internet Things J.* **2022**, *9*, 24009–24029. [\[CrossRef\]](#)

9. Qi, X.; Yuan, M.; Zhang, Q.; Yang, Z. Joint Power-Trajectory-Scheduling Optimization in a Mobile UAV-Enabled Network via Alternating Iteration. *China Commun.* **2022**, *19*, 136–152. [[CrossRef](#)]
10. Zhang, Y.; Gong, Y.; Guo, Y. Energy-Efficient Resource Management for Multi-UAV-Enabled Mobile Edge Computing. *IEEE Trans. Veh. Technol.* **2024**, *73*, 12026–12037. [[CrossRef](#)]
11. Li, X.; Qin, Y.; Huo, J.; Huangfu, W. Computation Offloading and Trajectory Planning of Multi-UAV-Enabled MEC: A Knowledge-Assisted Multiagent Reinforcement Learning Approach. *IEEE Trans. Veh. Technol.* **2024**, *73*, 7077–7088. [[CrossRef](#)]
12. Zeng, Y.; Chen, S.; Li, J.; Cui, Y.; Du, J. Online Optimization in UAV-Enabled MEC System: Minimizing Long-Term Energy Consumption Under Adapting to Heterogeneous Demands. *IEEE Internet Things J.* **2024**, *11*, 32143–32159. [[CrossRef](#)]
13. Pan, Y.; Zhang, S.; Wang, L. Cooperative trajectory planning and resource allocation for UAV-enabled integrated sensing and communication systems. *IEEE Trans. Veh. Technol.* **2024**, *73*, 6502–6516. [[CrossRef](#)]
14. Hao, H.; Xu, C.; Zhang, W.; Yang, S.; Muntean, G.-M. Joint task offloading, resource allocation, and trajectory design for multi-UAV cooperative edge computing with task priority. *IEEE Trans. Mob. Comput.* **2024**, *23*, 8649–8663.
15. Kota, N.R.; Naidu, K. Minimizing energy consumption in H-NOMA based UAV-assisted MEC network. *IEEE Commun. Lett.* **2023**, *27*, 2536–2540.
16. Diao, X.; Zheng, J.; Wu, Y.; Cai, Y.; Anpalagan, A. Joint trajectory design, task data, and computing resource allocations for NOMA-based and UAV-assisted mobile edge computing. *IEEE Access* **2019**, *7*, 117448–117459.
17. Liu, S.; Huang, Y.; Hu, H.; Si, J.; Kang, Q.; Pan, Y.; Gu, C. Minimizing energy consumption in UAV assisted NOMA-MEC networks. *Phys. Commun.* **2023**, *60*, 102167.
18. Liu, Z.; Liu, X.; Leung, V.C.M.; Durrani, T.S. Energy-Efficient Resource Allocation for Dual-NOMA-UAV Assisted Internet of Things. *IEEE Trans. Veh. Technol.* **2023**, *72*, 3532–3543. [[CrossRef](#)]
19. Budhiraja, I.; Kumar, N.; Tyagi, S.; Tanwar, S. Energy consumption minimization scheme for NOMA-based mobile edge computation networks underlying UAV. *IEEE Syst. J.* **2021**, *15*, 5724–5733. [[CrossRef](#)]
20. Qian, L.P.; Zhang, H.; Wang, Q.; Wu, Y.; Lin, B. Joint Multi-Domain Resource Allocation and Trajectory Optimization in UAV-Assisted Maritime IoT Networks. *IEEE Internet Things J.* **2023**, *10*, 539–552. [[CrossRef](#)]
21. Zhang, J.; Zhou, L.; Zhou, F.; Seet, B.-C.; Zhang, H.; Cai, Z.; Wei, J. Computation-efficient offloading and trajectory scheduling for multi-UAV assisted mobile edge computing. *IEEE Trans. Veh. Technol.* **2019**, *69*, 2114–2125. [[CrossRef](#)]
22. Liang, X.; Deng, Q.; Shu, F.; Wang, J. Energy-efficiency joint trajectory and resource allocation optimization in cognitive UAV systems. *IEEE Internet Things J.* **2022**, *9*, 23058–23071. [[CrossRef](#)]
23. Mei, W.; Zhang, R. Uplink cooperative NOMA for cellular-connected UAV. *IEEE J. Sel. Top. Signal Process.* **2019**, *13*, 644–656. [[CrossRef](#)]
24. Wang, B.; Liu, K.J.R. Advances in cognitive radio networks: A survey. *IEEE J. Sel. Top. Signal Process.* **2011**, *5*, 5–23. [[CrossRef](#)]
25. Siva, D.M.; Lin, X.; Helka-Liina, M.; Jonas, S.; Zou, Z. An overview of 3GPP Release-15 study on enhanced LTE support for connected drones. *IEEE Commun. Stand. Mag.* **2019**, *5*, 140–146.
26. Yang, Z.; Liu, Y.; Chen, Y.; Al-Dhahir, N. Cache-aided NOMA mobile edge computing: A reinforcement learning approach. *IEEE Trans. Wirel. Commun.* **2020**, *19*, 6899–6915. [[CrossRef](#)]
27. Azarhava, H.; Niya, J. M. Energy efficient resource allocation in wireless energy harvesting sensor networks. *IEEE Wirel. Commun. Lett.* **2020**, *9*, 1000–1003. [[CrossRef](#)]
28. Hua, M.; Wang, Y.; Li, C.; Huang, Y.; Yang, L. Energy-efficient optimization for UAV-aided cellular offloading. *IEEE Wirel. Commun. Lett.* **2019**, *8*, 769–772. [[CrossRef](#)]
29. Ding, Z.; Ng, D.W.K.; Schober, R.; Poor, H.V. Delay minimization for NOMA-MEC offloading. *IEEE Signal Process. Lett.* **2018**, *25*, 1875–1879. [[CrossRef](#)]
30. Mei, H.; Yang, K.; Liu, Q.; Wang, K. 3D-trajectory and phase-shift design for RIS-assisted UAV systems using deep reinforcement learning. *IEEE Trans. Veh. Technol.* **2022**, *71*, 3020–3029. [[CrossRef](#)]
31. Grant, M. CVX: MATLAB Software for Disciplined Convex Programming, Version 1.21. 2011. Available online: <http://cvxr.com/cvx> (accessed on 10 May 2024).
32. Wang, T.; Fang, F.; Ding, Z. An SCA and relaxation based energy efficiency optimization for multi-user RIS-assisted NOMA networks. *IEEE Trans. Veh. Technol.* **2022**, *71*, 6843–6847. [[CrossRef](#)]
33. Agrawal, A.; Barratt, S.; Boyd, S. Learning convex optimization models. *IEEE/CAA J. Autom. Sin.* **2021**, *8*, 1355–1364. [[CrossRef](#)]
34. Diao, X.; Wang, M.; Zheng, J.; Cai, Y. Fairness-aware offloading and trajectory optimization for multi-UAV enabled multi-access edge computing. *IEEE Access* **2020**, *8*, 124359–124370. [[CrossRef](#)]
35. Li, L.; Wen, X.; Lu, Z.; Jing, W. An energy efficient design of computation offloading enabled by UAV. *Sensors* **2020**, *20*, 3363. [[CrossRef](#)] [[PubMed](#)]

Disclaimer/Publisher’s Note: The statements, opinions and data contained in all publications are solely those of the individual author(s) and contributor(s) and not of MDPI and/or the editor(s). MDPI and/or the editor(s) disclaim responsibility for any injury to people or property resulting from any ideas, methods, instructions or products referred to in the content.